DEVELOPMENT OF ELECTRON SPIN POLARIZATION IN PHOTOSYNTHETIC ELECTRON TRANSFER BY THE RADICAL PAIR MECHANISM

RICHARD FRIESNER, G. CHARLES DISMUKES, AND KENNETH SAUER,
Laboratory of Chemical Biodynamics, Lawrence Berkeley Laboratory, and Department of Chemistry, University of California, Berkeley, California 94720 U.S.A.

ABSTRACT We have extended the radical pair theory to treat systems of membrane-bound radicals with g tensor anisotropy. Analysis of the polarized electron paramagnetic resonance (EPR) signals of $P700^+$, originating from photosystem I of higher plants, in terms of the radical pair mechanism provides information about the sequence of early electron acceptors. To account for the orientation dependence of the line shape and integrated area of this polarized signal, we propose the electron transfer sequence to be $P700 \rightarrow A_1 \rightarrow X \rightarrow Fd(A, B)$, where A_1 is a small organic molecule (possibly chlorophyll), X is the acceptor species observed recently in low-temperature EPR studies, and Fd(A, B) are the ferredoxin iron-sulfur centers A and B. Our calculations provide information about the lifetimes of A_1^-, and X^-, and their exchange interactions with $P700^+$. We also find supporting evidence for the orientation of X^- in the thylakoid membrane reported recently by G. C. Dismukes and K. Sauer (*Biochim. Biophys. Acta.* **504**:431-445.).

INTRODUCTION

In two preceding papers (1, 2) (hereafter designated as I and II, respectively) we reported the observation of a polarized electron paramagnetic resonance (EPR) signal from spinach chloroplasts arising from photosystem I. It was proposed in paper II that this signal is produced by a non-Boltzmann distribution of spins of the cation radical of P700, the primary electron donor of photosystem I.

In this paper we propose a model for the development of spin polarization in $P700^+$ that quantitatively explains the results reported in paper II. The model is based on the radical pair theory (3, 4), which has succeeded in accounting for chemically induced dynamic nuclear polarization (CIDNP) and electron polarization (CIDEP) in systems of freely diffusing radicals.

We extend the radical pair theory to include the effects of g tensor anisotropy, and incorporate modifications appropriate for a system of membrane-bound radicals. The results are qualitatively similar to those obtained for diffusive systems. For ordered immobilized radicals, g tensor anisotropy leads to a marked dependence of the intensity and sign of the polarization on orientation of the sample.

Conclusions about the initial photochemical events arise from application of this model to

---

Dr. Dismukes' present address is: Department of Chemistry, Frick Chemical Laboratory, Princeton University, Princeton, N. J. 08540.

photosystem I. Our results indicate that between P700 and P430 (ferredoxins A and B) two electron acceptors function in series under normal photosynthetic conditions. The first acceptor, which we shall call A_1, appears to be an organic molecule, possibly a chlorophyll. The anion radical of this species formed upon one electron reduction has an isotropic g tensor similar in magnitude to that of $P700^+$. The second acceptor, A_2, exhibits g tensor anisotropy and an orientation in the thylakoid membrane like that of the X^- species, observed previously in chloroplasts and membrane fragments under conditions of chemical reduction or intense illumination or both (5).

These conclusions agree with the interpretation of recent optical results of Sauer et al. (6). In those studies the kinetics of reduction of $P700^+$ after flash excitation in reduced photosystem I membrane fragments gave evidence of two acceptors preceding ferredoxins A and B.

EARLY EVENTS IN PHOTOSYSTEM I

The early electron transfer events in photosystem I of higher plants have been investigated primarily by EPR and optical spectroscopy. The initial step after the absorption of a photon is the transfer of an electron by the reaction center chlorophyll complex, designated P700 (7). The optical properties of P700 have been established, and the steady-state EPR spectrum of $P700^+$, signal I, can readily be observed upon illumination (8).

The reduced electron acceptor, which we shall refer to as A_1, forms a radical pair $P700^+—A_1^-$ with the oxidized reaction center species. Subsequently, the electron is transferred from A_1 to additional electron acceptors, ultimately reducing $NADP^+$.

Sauer et al. (6) have proposed the following acceptor scheme based on the kinetics of reduction of $P700^+$ after flash illumination: $P700 \rightarrow A_1 \rightarrow A_2 \rightarrow P430$. The species A_1 and A_2 were not seen directly by optical methods, but were detected indirectly from their effect on P700 absorption. The optical properties of P430, the only photoreduced species observed directly by optical methods, have been characterized by Ke (9).

Various EPR signals corresponding to reduced photosystem I acceptors have been reported in the literature. Table I lists the principal signals observed, their g tensor components, and midpoint potentials.

Electron acceptor centers A and B have been attributed to bound ferredoxin species (10), and they also correlate with P430 (13). X^- can be observed upon flash illumination when centers A and B are reduced, or by trapping during illumination and freezing (14). It has been inferred, therefore, that X is closer to P700 than is P430. In the scheme above, it seems likely that X is either A_1 or A_2.

The spin-polarized EPR signals reported in paper II are observed at very short (micro-

TABLE I

g TENSOR VALUES AND MIDPOINT POTENTIALS OF PHOTOSYSTEM I ELECTRON ACCEPTORS

Species	g_x	g_y	g_z	Midpoint potential	References
				mV	
X^-	1.78	1.90	2.09	−730	5, 12
Center A	1.87	1.95	2.05	−553, −530	10, 11
Center B	1.89	1.93	2.05	−594, −580	10, 11

second) times during flash illumination of the sample. The signals are observed from a variety of preparations containing photosystem I, including broken spinach chloroplasts. The presence of spin polarization indicates that the radical from which it arises has a non-Boltzmann population of spin states. The transient present at $g = 2.0026$ (where signal I is normally observed) undergoes significant line shape changes when the chloroplasts are oriented in a velocity gradient. The changes in line shape and amplitude with orientation provide a basis for deducing the mechanism of charge separation in photosystem I and the organization of the electron transport cofactors within the membrane.

THE RADICAL PAIR MECHANISM

The radical pair mechanism was originally proposed to explain the anomolous spin polarization that develops in radicals observed in solution after the creation of a radical pair or after a spin selective reaction. An early quantitative formulation was that of Adrian (15), which predicted a dependence of the polarization on the hyperfine states and g values of the two radicals. In this section we present a brief description of the essential features of the radical pair mechanism, following Adrian; in the following sections we adapt and apply these results to the photosynthetic system under consideration.

For the case of a radical pair created by electron transfer from an excited donor molecule (D) to an unexcited acceptor (A), we can write an approximate spin Hamiltonian as

$$\mathcal{H}_{RP} = \beta \mathbf{H}_0 \cdot [\mathbf{g}_D \cdot \mathbf{S}_D + \mathbf{g}_A \cdot \mathbf{S}_A] - J\left(2\mathbf{S}_D \cdot \mathbf{S}_A + \frac{1}{2}\right) + \sum_i A_i^{(D)} \mathbf{I}_i^{(D)} \cdot \mathbf{S}_D + \sum_j A_j^{(A)} \mathbf{I}_j^{(A)} \cdot \mathbf{S}_A. \quad (1)$$

where β is the Bohr magneton, $\mathbf{H}_0$ is the applied magnetic field, $\mathbf{g}_A$ and $\mathbf{g}_D$ are the g tensors of the acceptor and donor species, respectively, $\mathbf{S}_A$ and $\mathbf{S}_D$ are spin operators for the unpaired electrons on the donor and acceptor radicals, J is the magnitude of the isotropic exchange interaction between A and D, $\mathbf{I}_i^{(m)}$ is the spin operator for the i^{th} nucleus on molecule m (m = A, D), and $A_i^{(m)}$ is the isotropic hyperfine coupling constant for the ith nucleus on molecule m.

Eq. 1 neglects the dipolar spin-spin interaction and the anisotropic exchange and hyperfine terms. We assume that, to a first approximation, these terms are small enough to have a minimal effect on the fixed energy levels of the radical pair and on the spin polarization.

The eigenstates of the Hamiltonian Eq. 1 have been determined by Adrian for the case where $\mathbf{g}_A$ and $\mathbf{g}_D$ are isotropic (i.e. scalars). In the Appendix, it is shown that we obtain solutions analogous to those of Adrian, except that the spin states are quantized in the direction of the effective field

$$\mathbf{h}' = \mathbf{H}_0 \cdot (\mathbf{g}_A + \mathbf{g}_D) \quad (2)$$

The eigenstates are then linear combinations of the spin functions $|S\rangle$, $|T_{-1}\rangle$, $|T_{+1}\rangle$, and $|T_0\rangle$. We shall assume from this point onward that the radical pair is created initially from a singlet state. In the appendix, we demonstrate that the mixing of $|S\rangle$ with $|T_{\pm 1}\rangle$ has a negligible effect on the net polarization when the g tensor anisotropy is sufficiently small. Therefore, we adopt an S-T_0 basis set.

The solutions to Eq. 1 are then

$$\phi_1 = [(\omega + J)/2\omega]^{1/2} \mid S> + [(\omega - J)/2\omega]^{1/2} \mid T_0>$$
$$\phi_2 = [(\omega - J)/2\omega]^{1/2} \mid S> - [(J + \omega)/2\omega]^{1/2} \mid T_0>$$
$$E_1 = +\omega; \qquad E_2 = -\omega \tag{3}$$

where $\omega = (H_{AD}^2 + J^2)^{1/2}$ and H_{AD} is given by

$$H_{AD} = <S \mid \mathcal{H}_{RP} \mid T_0>$$
$$= \frac{1}{2}\beta \mathbf{H}_0 \cdot (\mathbf{g}_D - \mathbf{g}_A) \cdot \mathbf{z} + \frac{1}{2}\left(\sum_i A_i^{(D)} m_{iz}^{(D)} - \sum_j A_j^{(A)} m_{jz}^{(A)}\right). \tag{4}$$

$\mathbf{z}$ is a unit vector in the direction of $\mathbf{h}'$, $m_{iz}^{(m)}$ is the z component of nuclear spin of the i^{th} nucleus on molecule m, and E_1 and E_2 are the energies of ϕ_1 and ϕ_2, respectively.

The polarization of the donor radical, ρ, is obtained by following the time evolution of the spin wave function. For a time interval t during which J is constant, $\rho(t)$ is given by

$$\rho(t) = 2<\psi(t) \mid S_{Dz} \mid \psi(t)>$$
$$= [C_T(0)C_S^*(0) + C_T^*(0)C_S(0)]$$
$$\times \{\cos^2\omega t + [(H_{AD}^2 - J^2)/\omega^2]\sin^2\omega t\}$$
$$+ (iJ/\omega)[C_T(0)C_S^*(0) - C_T^*(0)C_S(0)]\sin(2\omega t)$$
$$+ 2(JH_{AD}/\omega^2)\sin^2\omega t[\mid C_S(0) \mid^2 - \mid C_T(0) \mid^2], \tag{5}$$

where $C_T(0)$, $C_S(0)$ are the coefficients of $\mid T_0>$ and $\mid S>$ for the spin wave function at the beginning of the time interval of constant J ($t = 0$). In the following sections, we use Eq. 5 to calculate the spin polarization predicted by two alternative models of our experimental system.

CIDEP OF MEMBRANE-BOUND RADICALS

The radical pair mechanism described in the previous section has been applied primarily to diffusive systems. In those systems the two radicals must diffuse apart and then reencounter one another for appreciable polarization to develop.

To simplify the ensuing calculations, we set $\mid C_S(0) \mid^2 = 1$, $\mid C_T(0) \mid^2 = 0$, corresponding to the assumption of creation of the radical pair from an initial singlet state (see the Discussion for the justification of this assumption in photosystem I). The results that follow could easily be generalized by retaining the terms dependent upon $C_S(0)$ and $C_T(0)$.

The simplified expression for the polarization during a time interval t of constant J is, from Eq. 5,

$$\rho(t) = (2H_{AD}J/\omega^2) \cdot \sin^2\omega t. \tag{6}$$

This expression will be larger than the thermal population difference ($\sim 10^{-3}$ at room temperature) only if H_{AD} and J are of comparable magnitude for a time interval $\sim\omega^{-1}$. Because ω^{-1} is typically of the order of 10^{-9} s, and the diffusion correlation time is $\sim 10^{-12}$ s,

this condition is ordinarily not satisfied for freely diffusing radicals in solution, and the net polarization upon initial separation of the radicals is negligible. After a reencounter, other terms in Eq. 5 become significant, and the polarization develops as described by Adrian's model.

We consider here a system in which the radical species are bound to a membrane at fixed sites. A radical pair is produced by transfer of an electron from a donor molecule (D) to an initial acceptor (A_1). The electron is then transferred to successive acceptors in a fixed sequence.

We shall assume that all of the electron transfers are irreversible. This assumption is not necessary, but it simplifies the calculations considerably. Then, transfer away of an electron is analogous to diffusion. However, there can be no "return" of the radical pair, and the development of polarization has an origin distinct from that of diffusive systems.

The development of spin polarization on D^+ is a consequence of the time evolution of the coupled spin wave functions of the unpaired electrons on D^+ and A_n^-. This process will change the polarization with time as long as there is a large enough exchange coupling, J_n, between D^+ and A_n^-. We therefore must consider the interaction of all radical pairs formed by successive electron transfer in which J_n is appreciable.

We will assume that J_n is 0 for $n \geq 3$, because $A_3 \ldots A_n$ are presumably too distant from D^+ to have a significant exchange coupling. Then there are two reasonable models for the development of polarization. The one-site model assumes that J_2 is also negligible, and that only the interaction within $D^+A_1^-$ need be considered. The two-site model assumes that both J_1 and J_2 are significant, and that the interaction between D^+ and A_2^- must be included in a calculation of the spin polarization.

One-Site Model

An acceptor radical A_n^- is characterized by a lifetime, τ_n, which determines the duration of the existence of the radical pair $D^+A_n^-$. (This is in fact the case in photosystem I, where $P700^+$ has a life $>30\,\mu s$, much longer than the lifetimes of either A_1^- or A_2^-). The probability that the radical pair will exist for time t is given by $(dt/\tau_n)e^{-t/\tau_n}$. The time-averaged polarization for the one-site model is then

$$\rho(\tau_1) = (2/\tau_1)\int_0^\infty e^{-t/\tau_1}\,(H_1J_1/\omega_1^2)\sin^2\omega_1 t\,dt,$$

$$= 4H_1J_1\tau_1^2/(1 + 4\omega_1^2\tau_1^2), \tag{7}$$

where H_1 is the off-diagonal matrix element H_{AD} for the radical pair $D^+A_1^-$, and $\omega_1 = (H_1^2 + J_1^2)^{1/2}$.

Eq. 7 predicts a large value for ρ for suitable values of J_1 and τ_1. This is possible because, in contrast to the diffusive system, τ_1 may well be of the order of ω_1^{-1}. Thus, if J_1 is of the order of H_1, Eq. 7 may attain values greatly in excess of the thermal population difference.

Two-Site Model

For this model we need to calculate the net polarization on D^+ after the electron leaves A_2. The spin wave function at the time of transfer to A_2 (i.e. immediately after the elec-

tron has left A_1) is given by

$$\psi_1(t_1) = |S\rangle \cdot [\cos(\omega_1 t_1) - i(J_1/\omega_1)\sin(\omega_1 t_1)] - i|T_0\rangle \cdot [(H_1/\omega_1)\sin(\omega_1 t_1)], \quad (8)$$

where t_1 is the duration of existence of $D^+ A_1^-$.

The polarization after the radical pair $D^+ A_2^-$ has existed for time t_2 can be found by obtaining the coefficients $C_S(t_1)$, $C_T(t_1)$ from Eq. 8 and substituting them into Eq. 5:

$$\begin{aligned}\rho(t_1, t_2) = {} & (2H_1 J_1/\omega_1^2)\sin^2\omega_1 t_1[1 - (2J_2^2/\omega_2^2)\sin^2\omega_2 t_2] \\ & + (J_2 H_1/\omega_1\omega_2)\sin(2\omega_1 t_1)\sin(2\omega_2 t_2) \\ & + (2H_2 J_2/\omega_2^2)\sin^2\omega_2 t_2[1 - (2H_1^2/\omega_1^2)\sin^2\omega_1 t_1]. \end{aligned} \quad (9)$$

By time-averaging over t_1 and t_2, we obtain

$$\begin{aligned}\rho(\tau_1, \tau_2) = {} & [4H_1 J_1 \tau_1^2/(1 + 4\omega_1^2\tau_1^2)] \cdot [1 - 4J_2^2\tau_2^2/(1 + 4\omega_2^2\tau_2^2)] \\ & + [4J_2 H_1 \tau_1\tau_2/(1 + 4\omega_1^2\tau_1^2)] \cdot [1/(1 + 4\omega_2^2\tau_2^2)] \\ & + [4H_2 J_2 \tau_2^2/(1 + 4\omega_2^2\tau_2^2)] \cdot [1 - 4H_1^2\tau_1^2/(1 + 4\omega_1^2\tau_1^2)]. \end{aligned} \quad (10)$$

ORIENTATION EFFECTS

We now investigate the effect of g tensor anisotropy on the expressions for the polarization derived in the previous section. The effect arises from the dependence of the matrix elements H_n on the orientation of the radicals in the applied magnetic field $\mathbf{H}_0$. We shall restrict ourselves to a situation where only one radical involved in the development of spin polarization on D^+ is anisotropic; the coordinate system defining the orientation is then chosen to be the principal axis system of the anisotropic species. $\mathbf{H}_0$ is specified by a magnitude, $|H|$, and the spherical polar angles θ and ϕ.

The polarization of a hyperfine line i of D^+ is an ensemble average over all possible orientations of the membrane-bound radical system with respect to $\mathbf{H}_0$;

$$\bar{\rho}_i = (2/\pi)\int_0^{\pi/2}\int_0^{\pi/2} \rho_i(\theta, \phi) P(\theta, \phi)\, d\theta d\phi, \quad (11)$$

where $P(\theta, \phi)$ is the probability that the radicals possess orientation (θ, ϕ) relative to $\mathbf{H}_0$, and $\rho_i(\theta, \phi)$ is the spin density developed on D^+ in hyperfine state i from either Eq. 7 or Eq. 10, with $H_n(\theta, \phi)$ given by Eq. 10a of the Appendix.

We anticipate the next section and assume that the g tensor of D^+ is predominantly isotropic. For the one site model, we assume that A_1 is anisotropic; then, substitution of Eqs. 7 and 10A into 11 yields, with suitable rearrangement,

$$\bar{\rho}_I \text{ (one site)} = \frac{8}{\pi}\tau_1^2 J_1 \cdot \left[\int_0^{\pi/2}\int_0^{\pi/2} \beta |\mathbf{H}_0| \Delta g_1(\theta, \phi) P(\theta, \phi)\, d\theta d\phi / I_1(\theta, \phi) + \frac{\alpha_i}{2}\int_0^{\pi/2}\int_0^{\pi/2} \frac{P(\theta, \phi)\, d\theta d\phi}{I_1(\theta, \phi)}\right], \quad (12)$$

where

$$\Delta g_n = -\tfrac{1}{2}[g_n^x \sin^2\theta\cos^2\phi + g_n^y \sin^2\theta\sin^2\phi + g_n^z \cos^2\theta - g_D]. \quad (13)$$

g_n^x, g_n^y, and g_n^z are the principal g tensor components of A_n^-, g_D is the isotropic g value of D^+, α_i is the total hyperfine field, $\sum_j A_j^{(D)} m_{jz}^{(D)}$, of D^+ in hyperfine state i, and $I_n(\theta, \phi) = 1 + 4\omega_n^2(\theta, \phi)\tau_n^2$.

Defining

$$U_n = \frac{2}{\pi} \beta \mid \mathbf{H}_0 \mid \int_0^{\pi/2} \int_0^{\pi/2} \Delta g_n(\theta, \phi) P(\theta, \phi) \, d\theta d\phi / I_n(\theta, \phi), \tag{14}$$

$$V_n = \frac{2}{\pi} \int_0^{\pi/2} \int_0^{\pi/2} d\theta d\phi \, P(\theta, \phi) / I_n(\theta, \phi), \tag{15}$$

we have

$$\bar{\rho}_i(\text{one site}) = 4\tau_1^2 J_1 (U_1 + \tfrac{1}{2}\alpha_i V_1). \tag{16}$$

For the two-site model, we again anticipate the next section and assume that the g tensor of only A_2^- is anisotropic, and that $g_1 = g_D$ are both scalars. Then, noting that $H_1 = \alpha_i/2$ (since $\Delta g_1 = 0$) and that both H_1 and ω_1 are orientation-independent, we obtain

$$\begin{aligned} \bar{\rho}_i(\text{two-site}) = (\alpha_i/2)\{&[4J_1\tau_1^2/(1 + 4\omega_1^2\tau_1^2)] \cdot (1 - 4J_2^2\tau_2^2 V_2) \\ &+ [4J_2\tau_1\tau_2/(1 + 4\omega_1^2\tau_1^2)] \cdot V_2 + 4\tau_2^2 J_2 V_2 \cdot [(1 - 4H_1^2\tau_1^2/(1 + 4\omega_1^2\tau_1^2)]\} \\ &+ 4U_2\tau_2^2 J_2 \cdot [1 - 4H_1^2\tau_1^2/(1 + 4\omega_1^2\tau_1^2)]. \end{aligned} \tag{17}$$

The experimental EPR intensity I_D of D^+ as a function of field position H is given by

$$I_D(H) = \sum_{\substack{\text{all hyperfine} \\ \text{configurations} \\ \text{of } D^+}} (-\bar{\rho}_i) e^{(H - H_i^0)^2/\delta^2} \tag{18}$$

where H_i^0 is the center of hyperfine line i, and δ is the half-width of the individual hyperfine lines. Note that a positive value of $\bar{\rho}_i$ results in a negative EPR intensity, i.e. $\bar{\rho}_i > 0$ means that hyperfine line i will be found in emission. This is the case because ρ is defined as $N_\alpha - N_\beta$, and an excess population of the state higher in energy (α) leads to a net emission of radiation.

In the next section, we examine the ability of Eqs. 16 and 17 to predict the intensity patterns of the signals observed in photosystem I and, thereby, deduce a mechanism for the development of this polarization.

CIDEP IN PHOTOSYSTEM I

Fig. 3 in paper II displays the CIDEP signals from flow-oriented and from randomly oriented broken spinach chloroplasts. The velocity gradient in the configuration of the EPR spectrometer orients the normal to the thylakoid membranes in the chloroplasts perpendicular to the applied magnetic field (2, 5).

Paper II presents arguments that the CIDEP signals from both the oriented and the unoriented systems are due to the $P700^+$ cation radical. We shall adopt this as a working hypothesis, supported by the calculations which follow.

The possible assignments of electron acceptors in photosystem I and the results of the previous section suggest two alternate schemes for the development of spin polarization: (*a*) Acceptor A_1 is the species X, and polarization develops as in the one-site model; (*b*) Acceptor A_1 is a small organic molecule, possibly Chl, and A_2 is X, and polarization develops as in the two-site model.

We have rejected two other conceivable schemes. A one-site model with Chl as A_1 would be inappropriate because it would not account for the orientation dependence of the polarized signal. A two-site model with X as A_1 and bound Fd (center A or B) as A_2 would fail to predict correctly the mixed emissive-enhanced absorptive pattern of the oriented signal for much the same reason as the one-site model (see the analysis of the one-site model for details): i.e., the term proportional to the hyperfine field of $P700^+$ would be too small.

It has been shown (5) that the x component of the g tensor of X^- (1.78) is oriented parallel to the short axis of the thylakoid membranes. Thus, the result of flow orientation is to align the g_x component normal to $\mathbf{H}_0$.

The effect of orientation upon the development of polarization can now be determined for the one and two-site models. The only orientation-dependent terms in Eqs. 16 and 17 are the integrals U_n and V_n. We first note that U_1(one-site) = U_2(two-site), and V_1(one-site) = V_2(two-site), since all of these integrals involve the g tensor components, lifetime, and J value of the same anisotropic species, X^-. We therefore drop the subscripts, and refer to these integrals as U and V, respectively.

For a random orientation (no flow, NF), $P(\theta, \phi) = \sin\theta$ for all θ, ϕ, and

$$U^{NF} = \frac{2}{\pi}\int_0^{\pi/2}\int_0^{\pi/2} \Delta g_X^{NF}\sin\theta\,d\theta d\phi/\{1 + 4\tau_X^2[J_X^2 + H_X^2(\theta,\phi)]\}, \tag{19}$$

where τ_X is the lifetime of X^-, J_X is the exchange interaction between $P700^+$ and X^-, $H_X = (\alpha_i/2) + \Delta g_X^{NF}$, and $\Delta g_X^{NF}(\theta,\phi) = -(1.78\sin^2\theta\cos^2\phi + 1.90\sin^2\theta\sin^2\phi + 2.09\cos^2\theta) + 2.0026$.

$$V^{NF} = \frac{2}{\pi}\int_0^{\pi/2}\int_0^{\pi/2} \sin\theta\,d\theta d\phi/[1 + 4\tau_X^2(J_X^2 + H_X^2)]. \tag{20}$$

For the flow-oriented system (F), we set $\phi = \pi/2$ [i.e. $P(\theta,\phi) = \delta(\phi - \frac{1}{2}\pi)$]. Then U and V are given by

$$U^F = \frac{2}{\pi}\int_0^{\pi/2} \frac{\Delta g_X^F(\theta)\,d\theta}{1 + 4\tau_X^2[J_X^2 + H_X^2(\theta)]}, \tag{21}$$

$$V^F = \frac{2}{\pi}\int_0^{\pi/2} \frac{d\theta}{1 + 4\tau_X^2[J_X^2 + H_X^2(\theta)]}, \tag{22}$$

where $\Delta g_X^F(\theta) = 1.90\sin^2\theta + 2.09\cos^2\theta - 2.0026$, and $H_X(\theta) = \Delta g_X^F(\theta) + \alpha_i/2$.

We have set g_D (the isotropic g value of the donor radical) equal to 2.0026, the experimental value for $P700^+$.

We can now evaluate the predictions for the polarized $P700^+$ line shape in the context of

the two models described above. There are three important experimental observations which a successful model must explain:

(*a*) The EPR spectrum from the unoriented sample is in total emission, i.e. the polarization is positive across the entire hyperfine field of $P700^+$. The signal from the oriented system displays a mixed emissive-enhanced absorptive pattern; the polarization changes sign near $\alpha_i = 0$.

(*b*) The integrated area ratio for either polarized signal to the relaxed $P700^+$ signal is approximately 13:1 (i.e., the population difference, $|N_\alpha - N_\beta|$, is more than 10 times the thermal value, 10^{-3}, at 300°K). Because relaxation has already begun when the EPR measurements are made, the calculated area ratios should be in excess of 13:1.

(*c*) The area ratio of the unoriented signal to the oriented signal is between 1:1 and 2:1 (this number is at present experimentally uncertain).

One-Site Model

We make the simplifying approximation that $|\Delta g_1| + |J_1| \gg |\alpha_i/2|$, since α_i for P700+ is typically a few gauss (the peak-to-peak line width of the steady-state $P700^+$ signal is 7.5 G). Then, $\omega_1^2 \sim (\Delta g_1)^2 + J_1^2$, and we can write Eq. 16 as

$$\bar{\rho}_i(\text{one-site}) = k_1[\alpha_i + \Delta g_1], \tag{23}$$

where $k_1 = 2V\tau_1^2 J_1$, and $\Delta g_1 = 2U/V$.

The Δg_1 term is mathematically isomorphic to the g value difference term in Adrian's original formulation. Both k_1 and Δg_1 are independent of α_i.

The orientation dependence of Eq. 21 is easily described. The integral U decreases by a factor of 10–100 upon orientation, i.e. $10 < U^{NF}/U^F < 100$. The integral V is relatively insensitive to orientation, $V^{NF}/V^F \sim 1$ for a wide range of τ_1 and J_1. Thus, $k_1^{NF}/k_1^F \sim 1$, and $10 < \Delta g_1^{NF}/\Delta g_1^F < 100$. The absolute amplitudes of Δg_1^{NF} and k_1 depend upon the specific values of τ_1 and J_1.

The one-site model correctly predicts the unoriented signal to be in total emission. Δg_1^{NF} is large and positive, the net polarization of the signal is sufficiently greater than the thermal population difference to account for the 13:1 area ratio of the polarized to unpolarized signal.

However, the one-site model fails completely for the oriented signal. The integral V is always small; therefore, k_1 is always small, less than 0.0025. Since Δg_1 is inversely proportional to k_1, the hyperfine term α_i is dominated by Δg_1 even for the oriented system. Furthermore, the total polarization for the oriented system is insufficient to account for the observed area ratios. Even for the most favorable values of τ_1 and J_1, the one-site model predicts that the oriented signal is much smaller than the unoriented signal (a factor of 10 or more) and in total emission. We therefore conclude that the one-site model cannot explain our results.

Two-Site Model

The polarization equation for the two-site model can be written as

$$\bar{\rho}_i(\text{two site}) = k_2(\alpha_i + \Delta g_2), \tag{24}$$

where $k_2 = 2J_1\tau_1^2/(1 + 4\omega_1^2\tau_1^2) + V \cdot \{2\tau_1^2 J_2 + [2\tau_1 J_2 \tau_2/(1 + 4\omega_1^2\tau_1^2)](1 - J_1 J_2 \tau_1 \tau_2)\}$, and $\Delta g_2 = 2U\tau_2^2 J_2/k_2$.

We have assumed that $|\alpha_i| \ll |J_1|$ and $|\alpha_i| \ll \Delta g_2$, so that ω_1, ω_2 are independent of α_i, and the term $[4H_1^2\tau_1^2/(1 + 4\omega_1^2\tau_1^2)] \ll 1$ in Eq. 17 and thus has been neglected. Both k_2 and Δg_2 are then independent of α_i.

The major difference between the one- and two-site models is the amplitude of k. k_1 is directly proportional to the integral V, which is small for all values of τ_X and J_X. k_2 is a sum of two terms, one proportional to V and one independent of V. It is the latter term, $2J_1\tau_1^2/(1 + 4\omega_1^2\tau_1^2)$, which can have a relatively large amplitude for appropriate values of τ_1 and J_1. This term arises from the interaction between $P700^+$ and A_1^-, and is large because Δg_1 is zero, so that $H_1 \ll J_1$. Effectively, the interaction of $P700^+$ with A_1^- produces a substantial polarization term proportional to the hyperfine field of $P700^+$. The corresponding term in the one-site model is small because the only radical pair interaction available is $P700^+ — X^-$. For this radical pair, the g value difference is quite large relative to α_i for almost all orientations of X^-.

The experimental signals can be generated from Eq. 24 when k_2 is sufficiently large (so that the polarized signals have enough amplitude relative to the relaxed signal) and when the average value of α_i (2–3 G) falls between Δg_2^f and Δg_2^{NF}. Then, for the oriented system the term linear in α_i dominates, the sign of $\bar{\rho}_i$ is governed by the sign of α_i, and a mixed emissive-enhanced absorptive signal results. For the unoriented system, the sum $(\alpha_1 + \Delta g_2)$ is positive for all values of α_i, and the polarized signal is seen in total emission.

In the next section, we simulate the polarized signals quantitatively by substituting Eq. 24 into Eq. 18 and summing over all configurations of the $P700^+$ hyperfine system.

RESULTS OF CALCULATIONS WITH THE TWO-SITE MODEL

We first calculated an EPR spectrum for an isolated, relaxed $P700^+$ radical, assuming that it is an oxidized chlorophyll dimer (16). The relative amplitudes of the hyperfine coupling constants were from nuclear magnetic resonance (NMR) studies (17); the magnitudes were scaled to the electron nuclear double resonance (ENDOR) result for the largest coupling constant (18).

The narrowing of the polarized signal (see Discussion) was introduced phenomenologically by uniformly decreasing all of the hyperfine coupling constants until the experimental line width was reproduced. An identical adjustment was used to simulate the signal for both the oriented and unoriented systems.

Fig. 1 displays the dependence of the EPR line shape on the value of Δg_2 in Eq. 24. For $\Delta g_2 < 0.7$ G, a nearly symmetrical mixed emissive-enhanced absorptive pattern results. For $\Delta g_2 > 4$ G, the signal is essentially in total emission. For $0.7 \text{ G} < \Delta g_2 < 4$ G, a line shape intermediate between the two previous cases is found.

The integrated area of a polarized signal depends linearly on k_2, and in a complicated fashion upon Δg_2. Table II lists the integrated area of $|I(\mathbf{H})|$ as a function of Δg_2; the area of the unpolarized signal is set equal to 1.0, and the polarized signals are normalized to this. The net integral area relative to the thermal equilibrium value for signal I at 300°K is found by multiplying the value in Table II by $k_2/0.001$ (0.001 is the thermal population difference at 300°K).

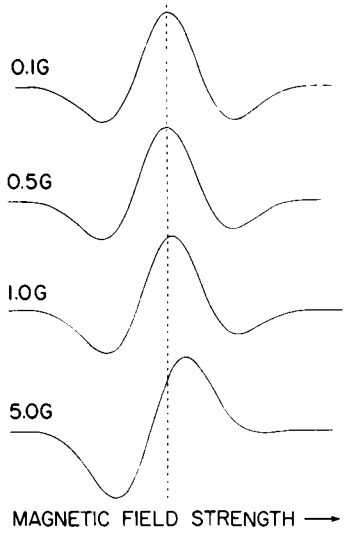

FIGURE 1

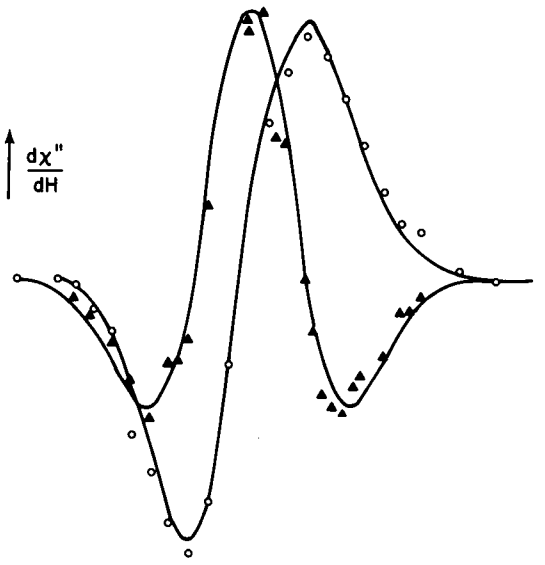

FIGURE 2

FIGURE 1 Simulated EPR spectra for the polarized signal for $\Delta g_2 = 0.1, 0.5, 1.0$, and 5.0 G.
FIGURE 2 Calculated and experimental EPR spectra for the oriented and unoriented polarized signal from spinach chloroplasts. Values of the parameters used in the simulation are $\tau_1 = 0.35$ ns, $\tau_2 = 35$ ns, $J_1 = 75$ G, $J_2 = 3.5$ G. Solid triangles (▲) are experimental intensities for flow-oriented chloroplasts. Open circles (○) are experimental intensities for unoriented chloroplasts (2). Solid lines are theoretical curves.

From these results we can set limits on k_2 and Δg_2 such that the three fitting criteria for the experimental signals described above are satisfied. The general line shape analysis requires that $0 < \Delta g_2^F < 0.7$ G, while $\Delta g_2^{NF} > 4$ G. Since the polarized signals have an area 3.5–6 times greater than that of the unpolarized signal when k_2 is set equal to 0.001, we require that $k_2/0.001 > 3.7$, so that the net area ratio is greater than 13:1. An upper limit of 2:1 on the area ratio of the oriented and unoriented polarized signals can be insured by setting the limit $\Delta g_2^{NF} < 6.5$ G.

The values of k_2, Δg_2^F, and Δg_2^{NF} are determined by the parameters τ_1, τ_2, J_1, and J_2.

TABLE II
RELATIVE AREA OF THE POLARIZED SIGNAL AS A FUNCTION OF Δg_2 (SIGNAL I = 1.0)

Δg_2	Area
0.0	3.6
0.1	3.6
0.2	3.6
0.5	3.6
1.0	3.7
2.0	4.0
5.0	6.0
10.0	10.5

TABLE III

CALCULATED VALUES OF k_2, Δg_2^F AND Δg_2^{NF} FOR SELECTED VALUES OF τ_1, τ_2, J_1 AND J_2.

J_1	J_2	τ_1	τ_2	k_2	Δg_2^F	Δg_2^{NF}	$A^F_{pol}/A_{sig.\,I}$	A^{NF}/A^F
G	*G*	*ns*	*ns*	G^{-1}	*G*	*G*		
10	75	1.0	2.1	0.029	0.45	5.7	106	1.84
50	10	0.35	0.35	0.0046	0.29	5.3	16.6	1.74
50	20	1.0	1.0	0.0111	0.17	5.1	40.0	1.69
100	10	0.35	0.35	0.0045	0.28	5.0	16.6	1.67
100	10	1.0	2.1	0.067	0.07	4.5	241	1.58
150	10	0.35	0.35	0.0039	0.33	6.0	13.1	1.92
150	20	1.0	0.35	0.0047	0.27	4.9	16.6	1.65
150	10	3.5	35	0.0047	0.076	6.4	16.9	2.02
100	150	0.35	0.035	0.0051	0.54	5.4	18.4	1.76
50	50	3.5	35	0.0128	0.08	4.5	46.1	1.58
75	3.5	0.35	35	0.0047	0.13	5.0	16.7	1.67

Area ratios are calculated from Table II.

Table III presents several sets of parameters for which k_2, Δg_2^F, and Δg_2^{NF} fall within the limits prescribed above. The exact values of the individual exchange energies or lifetimes are not critical; a small change in τ_n or J_n will produce a correspondingly small change in the simulated EPR spectrum.

It is clearly not possible to deduce the absolute magnitudes of any of the parameters from the data available at present. We can, however, set some limits on τ_1 and J_1. It is necessary that $\tau_1 \geq 250$ ps, and $J_1 < 200$ G, for k_2 to be greater than 0.0037. Once τ_1 and J_1 are fixed, a limited set of pairs (τ_2, J_2) will generate acceptable values of Δg_2^F and Δg_2^{NF}.

For a comparison of theory and experiment, we chose a value of τ_1 comparable to the lifetime of I^-, the initial acceptor observed in photosynthetic bacteria (19, 20). We also chose $J_1 > J_2$, because A_1 is presumably closer to $P700^+$. The resulting values of J_1 and J_2 are reasonable ones for exchange interactions between organic molecules separated by 5–25 Å (21). They are also within the neighborhood of exchange interactions observed between electron acceptors in photosynthetic bacteria (22).

Fig. 2 displays the theoretical and experimental EPR signals for the oriented and unoriented samples. The amplitudes of the theoretical signals, which are larger than the experimental signals, are reduced to account for the effects of relaxation. It is seen that excellent agreement is obtained within the limits of experimental error.

DISCUSSION

The two-site model successfully predicts most of the important features of the polarized signals arising from oriented and unoriented chloroplasts. Many of the values of τ_1, τ_2, J_1, and J_2 which generate the correct line shapes are consistent with what is known about early photosynthetic events. The model is relatively insensitive to the details of the calculations, i.e. small errors in the polarization function (as are introduced by neglect of S-$T_{\pm 1}$ mixing) would have a minimal effect on the predicted line shapes and area ratios.

We believe that our results provide compelling (although indirect) evidence for the existence of an acceptor in photosystem I preceding X. A radical pair mechanism with X as the

initial acceptor is inconsistent with the mixed emissive-absorptive line shape and relative area of the oriented signal. The presence of an earlier acceptor with an isotropic g value close to that of $P700^+$ provides a simple and satisfying explanation for these features. The most likely candidate for A_1 at present is chlorophyll, because it is known to be present in sufficient quantity in reaction center preparations, and Chl^- has the requisite g tensor properties. Also, the midpoint reduction potential of chlorophyll a is -0.78 V (vs. normal hydrogen electrode, in dimethylsulfoxide) (23), consistent with its role as an earlier acceptor than X. In analogy with photosynthetic bacteria, pheophytin might also be considered as a suitable candidate for A_1. However, Thornber et al. have found no pheophytin in enriched photosystem I preparations (24). We have no direct information concerning the chemical identity of A_1.

The assignment of X as A_2 is also supported by our results. The alignment of the high-field component of the g tensor of A_2 normal to the plane of the thylakoid membrane is required to produce the transformation from a totally emissive spectrum to a mixed emissive-enhanced absorptive spectrum upon orientation. Neither iron-sulfur signal (centers A or B) displays the proper orientation in the membrane to generate the observed line shape changes (5). The successful simulation of the oriented and unoriented signals, assuming that A_2 is X, is convincing evidence that this interpretation is valid.

Paper I proposed a triplet mechanism for the development of spin polarization. It now appears highly unlikely that this mechanism is the principal source of polarization. Under normal circumstances, the triplet mechanism cannot generate a mixed emissive-enhanced absorptive line shape (4). Furthermore, it would be impossible to account quantitatively for the orientation dependence of the signal. The triplet and radical pair mechanisms are the only theories proposed to date to explain chemically induced spin polarization. The model presented here thus appears to be the only reasonable explanation that fits the experimental results.

The radical pair theory as developed by Adrian appears to apply to membrane-bound systems of radicals; the fundamental generator of spin polarization is, as in diffusive systems, S-T_0 mixing. The simple approach taken in this paper provides an adequate explanation for the experimental results to date; however, more sophisticated treatments are possible and may be needed in the future. One could, for example, allow back transfer of an electron, or postulate more than one site for the electron in X, or investigate the possibility that at room temperature reduced or unreduced X may have appreciable unpaired spin density due to mixing in of low-lying excited spin states. Development along these lines may become profitable when more data are available.

We have assumed throughout our calculations that the initial radical pair state is a singlet. This can be justified qualitatively without invoking any EPR results. The initial state of P700* is surely a singlet. If the rate of electron transfer from P700* to A_1 is comparable to that observed in bacterial systems (<20 ps) (19, 20), there would not be enough time for intersystem crossing to a triplet state. Also, the unusual spin polarization of the reaction center triplet state in bacteria can be explained if electron transfer occurs from the excited singlet state (25). A spin flip as a consequence of electron transfer is quantum mechanically forbidden. We thus expect the radical pair to have initially the same singlet character as P700*.

For conditions involving an initial singlet state and $\Delta g > 0$ we must have $J = \frac{1}{2}(E_S -$

$E_T) > 0$ for the polarization to be emissive. The sign of J indicates that the energy of the singlet state of the radical pair must be greater than that of the triplet state. This ordering of singlet and triplet states is not the same as that usually found for neutral radicals, for which covalent bond interactions lead to a bonding singlet state and an antibonding triplet state. However, other factors may be important in determining the exchange interaction for weakly coupled ion pairs like those created in photosystem I. Quantum mechanical mixing in of the state ($D^* - A$) with the radical pair state $D^+ - A^-$ could result in a lowering of the triplet radical pair state relative to the singlet.[1] Alternatively, specific nonbonding orientations of the radicals would also lead to a reversal of the two levels (26). Finally, the dominant contribution to the exchange energy may well be due to superexchange (21). If this is the case, it would be difficult to make a priori predictions about the sign of J without detailed information about the exchange pathways between the radical species.

The narrowing of the polarized signal relative to the relaxed $P700^+$ signal is an interesting phenomenon, for which we currently have no completely satisfying explanation. The polarized signal from the unoriented sample has a peak-to-peak line width of 5.6 G, as compared to the value of 7.5 G measured for the relaxed $P700^+$ signal. The polarized signal from the oriented sample is the derivative of a mixed emissive-enhanced absorptive line shape, and therefore its line width cannot be compared directly with those of the other signals. However, good simulation of the oriented signal requires that the starting line width be narrowed to the value of 5.6 G found for the unoriented signal.

The above observations are not predicted by the simple radical pair mechanism presented here. The polarization is either a constant across the hyperfine field (Δg_2 large) or linear in $\alpha_i(\Delta g_2$ small). Neither of these polarization functions leads to a symmetrical narrowing of hyperfine envelope of the $P700^+$ signal. Furthermore, one would not expect the effect to be identical for the oriented and unoriented systems.

Paper II discusses several hypotheses concerning the narrowing phenomenon. Determination of the origin of the narrowing will require further experimental and theoretical work.

Many interesting areas of future research are suggested by this paper. Further EPR and optical experiments on photosystem I are needed to evaluate details of the two-site model, determine values for lifetimes and exchange interactions, and determine the identity of A_1. An approach similar to the one described here can also be applied to the CIDEP signals reported from photosynthetic bacteria (27).

We would also like to thank Dr. A. Pines for helpful discussions concerning the signal narrowing, and Doctors C. Blanchard and F. J. Adrian for useful comments about the manuscript.

This work was supported by the Division of Biomedical and Environmental Research of the U.S. Department of Energy, and National Science Foundation Grant PCM 76-5074.

Received for publication 7 April 1978 and in revised form 27 July 1978.

APPENDIX

The radical pair Hamiltonian given in Eq. 1 can be split into two parts

$$\mathcal{H}_{RP} = \mathcal{H}_D + \mathcal{H}_{OD}, \tag{1A}$$

[1] Adrian, F. J. Personal communication.

where

$$\mathcal{H}_D = \frac{1}{2}\beta \mathbf{H}_0 \cdot (\mathbf{g}_A + \mathbf{g}_D) \cdot (\mathbf{S}_A + \mathbf{S}_D) + J\mathbf{S}_A \cdot \mathbf{S}_D$$

$$+ \frac{1}{2}\left[\sum_i A_i^{(D)} \mathbf{I}_i^{(D)} + \sum_j A_j^{(A)} I_j^{(A)}\right] \cdot (\mathbf{S}_A + \mathbf{S}_D),$$

$$\mathcal{H}_{OD} = \frac{1}{2}\beta \mathbf{H}_0 \cdot (\mathbf{g}_D - \mathbf{g}_A) \cdot (\mathbf{S}_D - \mathbf{S}_A)$$

$$+ \frac{1}{2}\left(\sum_i A_i^{(D)} \mathbf{I}_i^{(D)} - \sum_j A_j^{(A)} \mathbf{I}_j^{(A)}\right) \cdot (\mathbf{S}_D - \mathbf{S}_A).$$

$\mathcal{H}_D$ is diagonal in the basis $\{|S>, |T_0>, |T_{+1}>, |T_{-1}>\}$, provided that the spin functions $|\alpha>$ and $|\beta>$ are quantized in the direction of the effective field

$$\mathbf{z} = (\mathbf{g}_A + \mathbf{g}_D) \cdot \mathbf{H}_0 / \| (\mathbf{g}_A + \mathbf{g}_D) \cdot \mathbf{H}_0 \| \tag{2A}$$

The radical pair eigenfunctions and energies depend upon the off-diagonal elements of the above basis set of the operator $\mathcal{H}_{OD}$. We now show that, for small g tensor anisotropy, the mixing of $|S>$ with $|T_{+1}>$ and $|T_{-1}>$ is of negligible importance, and an $\{|S>, |T_0>\}$ basis set is sufficient for calculation of the polarization. We also derive an approximate expression for the matrix element $<S|H_{OD}|T_0> \equiv H_{AD}$ as a function of orientation of radicals A^- and D^+.

We shall assume that the donor radical is isotropic, with scalar g value g_D. We choose as a coordinate system the principal axis system of the acceptor radical. Then

$$\mathbf{H}_0 = |\mathbf{H}| (\sin\theta \cos\phi, \sin\theta \sin\phi, \cos\theta) \tag{3A}$$

$$\mathbf{g}_A = \begin{bmatrix} g_A^x & 0 & 0 \\ 0 & g_A^y & 0 \\ 0 & 0 & g_A^z \end{bmatrix}, \quad \mathbf{g}_D = \begin{bmatrix} g_D & 0 & 0 \\ 0 & g_D & 0 \\ 0 & 0 & g_D \end{bmatrix}$$

We define

$$\bar{g}_A = \tfrac{1}{3}(g_A^x + g_A^y + g_A^z); \ \Delta x = \bar{g}_A - g_A^x;$$
$$\Delta y = \bar{g}_A - g_A^y; \ \Delta z = \bar{g}_A - g_A^z$$
$$g_+ = \bar{g}_A + g_D; \ g_- = g_D - \bar{g}_A \tag{4A}$$

We wish to calculate the matrix elements $<S|H_{OD}|T_0>$, $<S|H_{OD}|T_{+1}>$, and $<S|H_{OD}|T_{-1}>$. We first define

$$H_{OD} = H_{HF} + H_{\Delta g}, \tag{5A}$$

where

$$H_{HF} = \frac{1}{2}\left(\sum_i A_i^{(D)} \mathbf{I}_i^{(D)} - \sum_j A_j^{(A)} \mathbf{I}_j^{(A)}\right) \cdot (\mathbf{S}_D - \mathbf{S}_A),$$

$$H_{\Delta g} = \tfrac{1}{2}\beta \mathbf{H}_0 \cdot (\mathbf{g}_D - \mathbf{g}_A) \cdot (\mathbf{S}_D - \mathbf{S}_A).$$

Because we are interested in the spin polarization of the donor radical, we set the sum over the acceptor hyperfine field equal to its ensemble average, i.e.

$$\sum_j A_j^{(A)} m_j^{(A)} \rightarrow \left\langle \sum A_j^{(A)} m_j^{(A)} \right\rangle = 0 \tag{6A}$$

The nuclear spin operators $I_j^{(D)}$ are quantized in the direction of the effective field, **z**. Then

$$\langle S \mid H_{HF} \mid T_{\pm 1} \rangle = 0$$

$$\langle S \mid H_{HF} \mid T_0 \rangle = \frac{1}{2} \sum_j A_j^{(D)} m_j^{(D)}, \tag{7A}$$

where $m_j^{(D)}$ is the projection of $I_j^{(D)}$ on **z**.

The matrix elements of $H_{\Delta g}$ must now be evaluated. Substitution of Eqs. 3 A and 4 A into 5 A yields

$$\begin{aligned}\langle S \mid H_{\Delta g} \mid T_0 \rangle = {} & \tfrac{1}{2}\beta \mid \mathbf{H} \mid \{\cos^2\phi \sin^2\theta (g_+ - \Delta x)(g_- + \Delta x) \\ & + \sin^2\theta \sin^2\phi (g_+ - \Delta y)(g_- + \Delta y) + \cos^2\theta (g_+ - \Delta z)(g_- + \Delta z)\} \\ & \cdot \{\cos^2\phi \sin^2\theta (g_+ - \Delta x)^2 + \sin^2\theta \sin^2\phi (g_+ - \Delta y)^2 \\ & + \cos^2\theta (g_+ - \Delta z)^2\}^{-1/2}. \end{aligned} \tag{8A}$$

In general, the matrix elements $\langle S \mid H_{\Delta g} \mid T_{\pm 1} \rangle$ will be complex. Since we intend to show only that these matrix elements are a small perturbation, we compute the absolute magnitudes.

$$\mid \langle S \mid H_{\Delta g} \mid T_{\pm 1} \rangle \mid = \left[\frac{\beta}{2} \mid\mid (\mathbf{g}_D - \mathbf{g}_A) \cdot \mathbf{H}_0 \mid\mid^2 - (\langle S \mid H_{\Delta g} \mid T_0 \rangle)^2 \right]^{1/2}.$$

We now make the approximation $g_- \sim \Delta x, \Delta y, \Delta z \ll g_+$. Then algebraic manipulation of Eq. 8A leads to

$$\begin{aligned}\langle S \mid H_{\Delta g} \mid T_0 \rangle & \approx \tfrac{1}{2}\beta \mid \mathbf{H} \mid [g_- - (\cos^2\phi \sin^2\theta \Delta x + \sin^2\phi \sin^2\theta \Delta y + \cos^2\theta \Delta z)], \\ \mid \langle S \mid H_{\Delta g} \mid T_{\pm 1} \rangle \mid & \approx [(g_- - \Delta x)^2 \cos^2\phi \sin^2\theta + (g_- - \Delta y)^2 \sin^2\theta \sin^2\phi \\ & \quad + (g_- - \Delta z)\cos^2\theta - (\langle S \mid H_{\Delta g} \mid T_0 \rangle)^2]^{1/2} \end{aligned} \tag{9A}$$

This gives as a final expression for $\langle S \mid H_{OD} \mid T_0 \rangle$

$$\begin{aligned}\langle S \mid H_{OD} \mid T_0 \rangle \equiv H_{AD} = {} & \tfrac{1}{2} \Sigma A_j^{(D)} M_j^{(D)} + \tfrac{1}{2} \beta \mid \mathbf{H} \mid [g_D - (g_A^x \cos^2\phi \sin^2\theta \\ & + g_A^y \sin^2\phi \sin^2\theta + g_A^z \cos^2\theta)]. \end{aligned} \tag{10A}$$

We estimate the effects of $T_{\pm 1}$ mixing by calculating the ensemble average value

$$\begin{aligned}\langle\langle S \mid H_{\Delta g} \mid T_{\pm 1} \rangle\rangle = {} & \frac{2}{\pi} \int_0^{\pi/2} \int_0^{\pi/2} \langle S \mid H_{\Delta g} \mid T_{\pm 1} \rangle \sin\theta \, d\theta d\phi \\ & \approx [\tfrac{1}{3}(\Delta x^2 + \Delta y^2 + \Delta z^2)]^{1/2} \cdot \tfrac{1}{2}\beta \mid \mathbf{H} \mid . \end{aligned} \tag{11A}$$

Substitution of values of Δx, Δy, and Δz for the species X^- yields

$$\langle \mid \langle S \mid H_{\Delta g} \mid T_{\pm 1} \rangle \mid \rangle \approx \beta \mid \mathbf{H} \mid \cdot (0.13). \tag{12A}$$

The mixing coefficients, $C_{ST_{\pm 1}}$, are given to first order by

$$\begin{aligned} C_{ST_{\pm 1}} & \propto \mid \langle S \mid H_{OD} \mid T_{\pm 1} \rangle \mid / (E_S - E_{T_{\pm 1}}) \\ & = \beta \mid \mathbf{H} \mid (0.13)/g\beta \mid \mathbf{H} \mid \approx (0.0325). \end{aligned} \tag{13A}$$

This 3.25% mixing in of the $T_{\pm 1}$ states leads to an error of less than 3% in the calculated polarization.

REFERENCES

1. BLANKENSHIP, R., A. MCGUIRE and K.SAUER. 1975. Chemically induced dynamic electron polarization in chloroplasts at room temperature. Evidence for triplet state participation in photosynthesis. *Proc. Natl. Acad. Sci. U.S.A.* **72**:4943–4947.
2. DISMUKES, G. C., A. MCGUIRE, R. BLANKENSHIP, and K. SAUER. 1978. Electron spin polarization in photosynthesis and the mechanism of electron transfer in photosystem I. Experimental observations. *Biophys. J.* **21**:239–256; **22**:521.
3. WAN, J. K. S., and A. J. ELLIOT. 1977. Chemically induced dynamic magnetic polarization in photochemistry. *Accounts Chem. Res.* **10**:161–166.
4. FREED, J. H., and J. B. PEDERSEN. 1976. The theory of chemically induced dynamic spin polarization. *Adv. Magn. Res.* **8**:1–84.
5. DISMUKES, G. C., and K. SAUER. 1978. The orientation of membrane bound radicals: an EPR investigation of magnetically ordered spinach chloroplasts. *Biochim. Biophys. Acta.* **504**:431–445.
6. SAUER, K., P. MATHIS, S. ACKER, and J. A. VAN BEST. 1978. Electron acceptors associated with P700 in triton solubilized Photosystem I particles from spinach chloroplasts. *Biochim. Biophys. Acta.* **503**:120–134.
7. KOK, B. 1961. Partial purification and determination of the oxidation reduction potential of the photosynthetic chlorophyll complex absorbing at 700 nm. *Biochim. Biophys. Acta.* **48**:527–533.
8. BEARDEN, A. J., and R. MALKIN. 1977. Chloroplast photosynthesis: the reaction center of photosystem I. *Brookhaven Symp. Biol.* **28**:247–265.
9. KE, B. 1973. The primary electron acceptor of Photosystem I. *Biochim. Biophys. Acta.* **301**:1–33.
10. EVANS, M. C. W., S. G. REEVES, and R. CAMMACK. 1974. Determination of the oxidation-reduction potential of the bound iron-sulfur proteins of the primary electron acceptor complex of Photosystem I in spinach chloroplasts. *FEBS (Fed. Eur. Biochem. Soc.) Lett.* **49**:111–114.
11. KE, B., R. E. HANSEN, and H. BEINERT. 1973. Oxidation-reduction potentials of bound iron-sulfur proteins of Photosystem I. *Proc. Natl. Acad. Sci. U.S.A.* **70**:2941–2945.
12. KE, B., E. DOLAN, K. SUGAHARA, F. M. HAWKRIDGE, S. DEMETER, and E. R. SHAW. 1977. Electrochemical and kinetic evidence for a transient electron acceptor in the photochemical charge separation in Photosystem I. *In* Photosynthetic Organelles. *Plant Cell. Physiol. Suppl.* **3**:187–199.
13. KE, B., and H. BEINERT. 1973. Evidence for the identity of P430 of Photosystem I and chloroplast bound iron-sulfur protein. *Biochim. Biophys. Acta.* **305**:689–693.
14. MCINTOSH, A. R., and J. R. BOLTON. 1976. Electron spin resonance spectrum of species "X" which may function as the primary electron acceptor in Photosystem I of green plant photosynthesis. *Biochim. Biophys. Acta.* **430**:555–559.
15. ADRIAN, F. J. 1971. Theory of anomalous electron spin resonance spectra of free radicals in solution. Role of diffusion-controlled separation and re-encounter of radical pairs. *J. Chem. Phys.* **54**:3918–3923.
16. KATZ, J. J., and J. R. NORRIS, JR. 1973. Chlorophyll and light energy transduction in photosynthesis. *Curr. Top. Bioenerg.* **5**:41–75.
17. SANDERS, J. K. M., and J. C. WATERTON. 1976. The chlorophyll-a radical cation: determination of hyperfine coupling constants by nuclear magnetic resonance spectroscopy. *J. Chem. Soc. D. Chem. Commun.* 247–248.

17a. SANDERS, J. K. M., and J. C. WATERTON. 1978. Hyperfine coupling in chlorophyll radical cations. A nuclear magnetic resonance approach. *J. Am. Chem. Soc.* **100**:4044–4049.

18. SCHEER, H., J. J. KATZ, and J. R. NORRIS. 1977. Proton-electron hyperfine coupling constants of the chlorophyll a cation radical by ENDOR spectroscopy. *J. Am. Chem. Soc.* **99**:1372–1381.
19. KAUFMANN, K. J., P. L. DUTTON, T. L. NETZEL, J. S. LEIGH, and P. M. RENTZEPIS. 1975. Picosecond kinetics of events leading to reaction center bacteriochlorophyll oxidation. *Science (Wash. D.C.).* **188**:1301–1304.
20. HOLTON, D., M. W. WINDSOR, W. W. PARSON, and J. P. THORNBER. 1978. Primary photochemical processes in isolated reaction centers of *Rhodopseudomonas viridis*. *Biochim. Biophys. Acta.* **501**:112–126.
21. METZNER, E. K. 1974. Spin exchange in biradicals. Ph.D. thesis, University of California, Berkeley, Calif. LBL 3356. Lawrence Berkeley Laboratory, Berkeley, Calif.
22. PRINCE, R. C., D. M. TIEDE, J. P. THORNBER, and P. L. DUTTON. 1977. Spectroscopic properties of the intermediary electron carrier in the reaction center of *Rhodopseudomonas viridis*. *Biochim. Biophys. Acta.* **462**:467–490.
23. DRYHURST, G. 1977. Electrochemistry of Biological Molecules. Academic Press, Inc., New York. 412.

24. THORNBER, J. P., R. S. ALBERTE, F. A. HUNTER, J. A. SHIOZAWA, and K. S. KAN. 1977. *Brookhaven Symp. Biol.* **28**:132–148.
25. THURNAUER, M. C., J. J. KATZ, and J. R. NORRIS. 1975. The triplet state in bacterial photosynthesis: Possible mechanisms of the primary photo-act. *Proc. Natl. Acad. Sci. U.S.A.* **72**:3270–3274.
26. KAPTEIN, R. 1972. Chemically induced dynamic nuclear polarization. VIII. Spin dynamics and diffusion of radical pairs. *J. Am. Chem. Soc.* **94**:6251–6262.
27. HOFF, A. J., P. GAST, and J. C. ROMIJN. 1977. Time-resolved ESR and chemically induced dynamic electron polarization of the primary reaction in a reaction center particle of *Rhodopseudomonas sphaeroides* wild-type at low temperature. *FEBS (Fed. Eur. Biochem. Soc.) Lett.* **73**:185–190.